Remote Sensing of Land
Homepage: www.gathacognition.com/journal/gcj1
http://dx.doi.org/10.21523/gcj1

Original Research Paper

Bathymetry Mapping using Landsat ETM+ Data and Field Measurements for West Coast of Yemen

Mamdouh El-Hattab[1]*, Waddah Almogamal[2]

1. Institute of Environmental Studies and Research, University of Sadat City, Egypt.
2. Hydrographic Surveying Section, Al-Hodeida- Port Authority, Yemen.

Abstract

The bathymetry of coastal waters in the Red Sea coastal water is of the vital importance for shipping safety because of presence of navigational hazards. We used remote sensing data from Landsat-7 (ETM+) for bathymetric mapping in Al-Luhaia port, Western Yemen. We used a global positioning system to locate the accurate sampling points for sea depth. An echo sounder was used to collect sea depth information. We examined suitability of wavelength bands for bathymetry. This paper puts forward a method to extract water depth information from multispectral data Landsat-7 (ETM+). We applied simple linear regression to relate field measured water depths to pixel brightness values in the blue band of Landsat-7 (ETM+) multispectral imagery that had been corrected to at-satellite reflectance using published calibration coefficients. The regression relationship at the clear shallow water site was accurate (R2 = 94.40% band 1) for water depths in the range 2 to 9m. The regression analysis offered by the model has been verified using data from 1500 points (depths) that were not used in model generation, were used for testing the validity. This validation test model offered a very good correlation coefficient, 0.9385. We made a comparison between actual depth measured by hydrographic echo sounder during the field measurement and the estimated depth derived from satellite images to establish the margins of error in the estimates. A mean of error of 4.08%, with an accuracy of 95.92% was found.

Article history

Received: 10 November, 2019;
Final form: 23 January 2020;
Accepted: 08 February 2020.

Keywords

Bathymetry;
Navigation;
Landsat;
ETM+;
Red Sea;
Yemen.

Editor(s)

Carlos Antonio da Silva Junior

1 INTRODUCTION

Nowadays, the hydrographic survey used in ocean environment in many aspects. Red Sea with its famous coral reefs has an irregular bottom especially in coastal zone, thus the bathymetry is of vital significance for shipping safety. The conventional hydrographic surveying or measuring the water depth is accurate for point measurement (Li-Guang *et al.*, 2005). Although typical methods of mapping bathymetry like ship-borne echo sounder (single or multi beam) provide accurate measures, but it unfortunately, need a lot of efforts and money especially for big areas (Hesselmans, 2000). Satellite images could use for mapping the areas as an alternative method. That method is capable for mapping the coastal waters bathymetry at any environments. The main disadvantage of using remote sensing for bathymetry measures is the mutable sea bottom effects on its readings (Pang *et al.*, 2004). Thus, the using of remote sensing for mapping bathymetry considered as a very promising tool, as it yield a synoptic view over huge ranges at low cost (Hesselmans *et al.*, 2000).

Optical remote sensing methods penetrate into the clear waters to up to fifteen to thirty meters. The electromagnitic waves penetrate sea water according to its wave length. The higher penetrating wave length is the blue (400nm), followed by red wavelengths (600nm). In addition to the wave length, there are also the optical properties of the water like organic matter and suspended sediments could affect the penetration (Stumpf *et al.*, 2003; Mumby *et al.*, 2004).

Many authors identified the uses of satellite data for measuring shallow water bathymetry, one of the satellite sensors used is Landsat Thematic Mapper (TM) sensor (Smith and Baker, 1981). Several remote sensing

* Author address for correspondence
Institute of Environmental Studies and Research, University of Sadat City, Egypt.
Tel.: +20 122346149
Emails: mmelhattab@gmail.com (*M. El-Hattab* -Corresponding author); waddahalmogamal@gmail.com (*W. Almogamal*).

https://dx.doi.org/10.21523/gcj1.19030103

satellites have a specific sensor that can be used for water condition study such as ocean color, coral reef mapping, and sedimentation spreading extent. One kind of satellite that has a capability in water condition study is Land Satellite using optic sensor to detect various electromagnetic long waves that started from visible light wave, infrared (near and medium) and thermal waves (Hesselmans *et al.*, 1997).

The satellite sensor depth estimation depends on the quantity of reflected light (that affected by many parameters like water clarity, depth diminution, bottom reflectance, suspended solids) (Baban, 1993). In comparison with field survey, the satellite images could use for mapping bathymetry more effective due to its global coverage, availability and low cost.

Many authors discussed the success using of different electromagnetic wave lengths in bathymetry studies (like Warne, 1972; Yi and Li, 1988; Kumar *et al.*, 1997; and George, 1997). The optimum water conditions for achieving the bathymetry detection by satellite sensors were discussed (Polcyn and Lyzenga, 1979). Selection of optimum wave lengths used in bathymetry studies depends on the type of water environment, as the lake water different completely from estuary water or sea water.

Modeling of bathymetry was achieved by different authors using a specific regression analysis model (Stove, 1985, Ibrahim and Cracknell, 1990; Baban 1993; Diaz *et al*., 2019; Tripathi and Rao, 2002). Benveniste *et al.*, (2019) and Wu *et al.*, (2018) obtained the requirements for a Coastal Hazards Observing System. Many authors used Landsat sensors with its specific resolution data for studying reefs and shallow water environments and its changes (like, Luczkovich *et al.*, 1993; Zainal *et al*., 1993; Holden and LeDrew, 1998; Andréfouët *et al*., 2001; Lubin *et al.*, 2001; Hochberg *et al*., 2003; Yamano and Tamura, 2004; Ji, 2008).

Bathymetry based on passive optical remote sensing uses sunlight. This light penetrates into the water and maybe reflected by the bottom. As the light moves through water column, it is absorbed and scattered by substances in the water. We ascribe absorption and scattering to suspend and dissolved materials in the water; chlorophyllous material, and the colored organic material components. The bottom reflectance depends on the sediment (sand-mud) and whether vegetation is present. If the path length of the light through the water increases, more light is absorbed. Therefore, bright areas indicate shallow water zones, whereas dark areas show deeper water. We have proposed several methodologies in the past to translate optical image data to bottom topography. Lyzenga (1978) derived an exponential relation between the height of the water column and the measured irradiance levels (Hesselmans *et al.*, 1997).

The principal goal of this work concerned to establish a new tool to reduce both efforts and money spent in producing bathymetry maps by traditional methods. That not mean we will exclude the traditional methods, but it will reduce trip's numbers needed to cover the coastal zones.

2 RESOURCES AND APPROACHES

In this section different resources and approaches used to achieve objectives will discussed in details.

2.1 Study Area

Al-Luhaia City is about 137 km north of Al-Hodeida and 20 km east of Antofash Island. The area of study location is north of Al-Luhaia town and is used by fishermen as a yard for their boats, it characterized by its important geographical position and by the bottom topography, and it covers an area 4.5 km (E) by 4.2 km (N). The approximate site center coordinates are 15°44′ 12.94887" N and 42°41' 33.36366" E (Figure 1). The availability of images by their geographical location and partly by the bottom topography partly governed the choice of this area.

2.2 Field Measures

All marine field survey was achieved by the 'Egyptian Hydrographic Company (Ehco) and Zone Engineering and Survey' carried out for an approximate area of 5.0 km × 4.0 km in May 2003 using a Differential GPS (DGPS) system.

High accuracy range (±5 cm) was used the reason of using such accuracy is that to get precise position for depth measurements moreover for mapping accurate coastline. We used bathymetric measurements the Echo-Sounder device type NaviSound 205 and the Software which was used is Trimble (HydroPro). We have collected more than 4000 observations from the study area during one long working day under suitable weather conditions (average Temperature 27 ºC); these reading data comprise digital easting/northing/depth triplets as recorded by the navigation system DGPS and sounding equipment on a vessel. Soundings in the area used range from less than one meter down to a little over 9 m and are fairly well distributed throughout the range. The data then tested and filtered from unessential reading, the useful data then used for analyzing. Survey and field measurements have been done for Al-Luhaia Site and carried out for an approximate area of 5.0 km x 4.0 km. The sound measures were corrected to mean sea level (MSL). Depth value measured at any point was added to the tide value at that specific date and time (0.11 m).

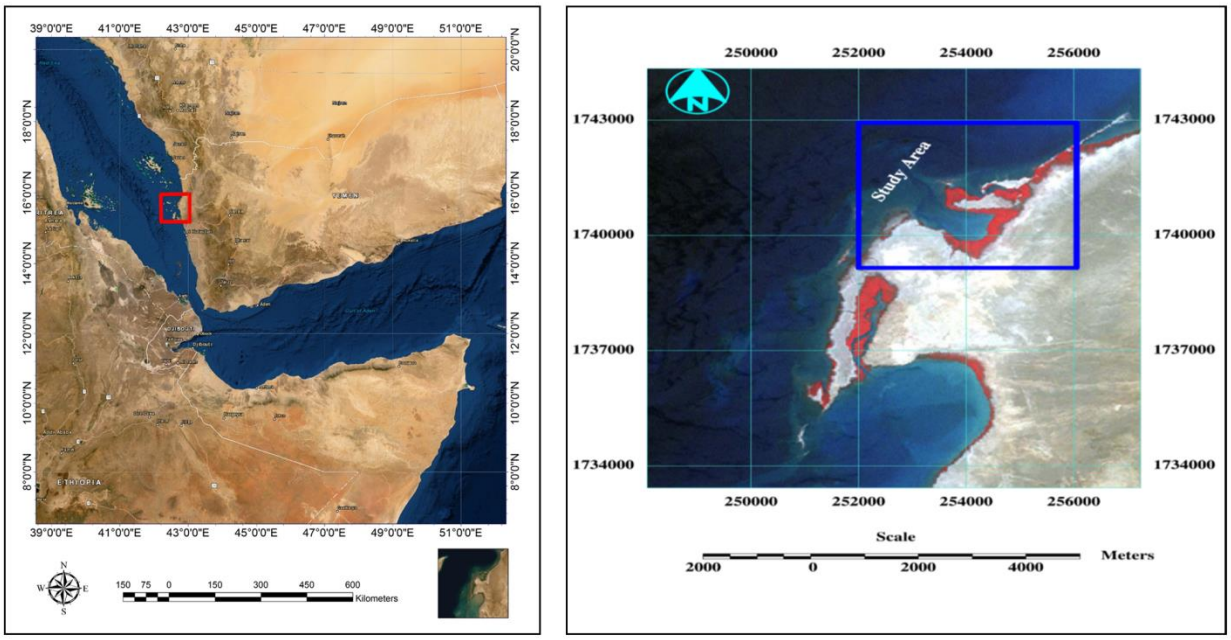

Figure 1. Study area [Color Composite Images]

2.3 Landsat ETM+ imagery

The images for the Al-Luhaia, main study area comprises path 167 row 49 in the Landsat Worldwide Reference System (WRS) (Figure 1). The image-base underlying this paper comprised Landsat-7 (ETM+) 8-Bit multispectral satellite imagery (06-02-2003) with nine different bands. The sensor pixel size is 28.5 meters for used spectral bands. The thermal infrared has a pixel size 60 m, it used to map the coast and line and merged islands also it can be useful for studying the surface features, whereas the visible bands provide the best water penetration. The ETM+ image characteristic for the Al-Luhaia study area can be explained in table 1.

3 DATA PROCESSING

Data processing and analysis moves through several steps. First, the image ordered from the United States Geological Survey (USGS) was geo-referenced but not satisfied to achieve the bathymetry depths that correlate to the DN values. As illustrated in figure 2, it's clear that the regression and correlation values (R^2 = 0.029 & R = 0.171%) revealed a very weak relationship between values of image digital numbers (DNs and water depth values measured directly through field survey, whilst after the re-registration for the same image band 1, a not bad improvement for regression and correlation relationship (R^2 = 0.214 and R = 0.463) revealed between DNs and water depth measurements as shown in figure 3, therefore it should re-register the images with the field water depth measurements.

As result of two different registration procedures 1st and 2nd polynomial orders that were used and show that the regression values (R^2) were higher for the bands in 1st polynomial order registration than 2nd order, therefore the all analysis were carried out by using 1st polynomial registration image. Table 2 shows the regression and correlation coefficients for the two methods that were used.

Second, as the image original digital number values have variances could affect the obtained result. The used image pixels values were averaging using low-pass filter to remove any anomalies. Several tests of low-pass ($3 \times 3, 5 \times 5, 7 \times 7$ and 9×9) filtering, or averaging of DN values, were applied. Table 3 shows the best filter, low-pass used for all bands and the regression and correlation values. The filter of size 5×5 represents the optimum filter window size. Blue, Green, and Red bands show the best fit, respectively. This shows that relationship is rather strong and was found to agree well (regression and correlation coefficients of 0.876 and 0.936).

We converted digital numbers to units of calibrated reflectance to calibrate images to surface reflectance. The overall accuracy for image shows improvement after the application of the DN converting to reflectance. Table 3 shows increasing in results between relationships of overall reflectance bands in the visible range with field depth that shows a model can estimate depths. A comparison of these results shows higher values in regression and correlation coefficients than the results that were obtained from low-pass filter 5×5 process, for example reflectance band 1 shows the regression results (0.944) while band 1 low-pass filter 5×5 gives (0.876). So we conclude that we should convert images to reflectance before any kind of analysis is taking place.

Table 1. ETM+ image

Characteristics	Descriptions
Acquisition date/time	06/02/2003
Sun angle azimuth	134.4741123 degrees
Sun angle elevation	46.0111028 degrees
File format	TIFF
Interpolation method	Nearest Neighbor
Datum	WGS 1984
Projection	UTM
Zone number	38
Percent cloud cover	0

Table 2. The regression and correlation results for procedures 1st and 2nd polynomial orders

	Polynomial 1		Polynomial2	
	Regression	Correlation	Regression	Correlation
Band 1(blue)	0.7974	0.8930	0.7826	0.8846
Band 2(green)	0.6992	0.8362	0.6981	0.8355
Band 3(red)	0.4754	0.6895	0.5010	0.7078

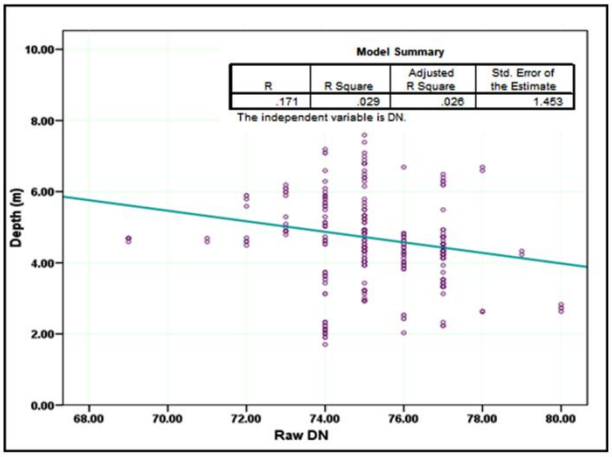

Figure 2. Raw DN of band1 before rectification

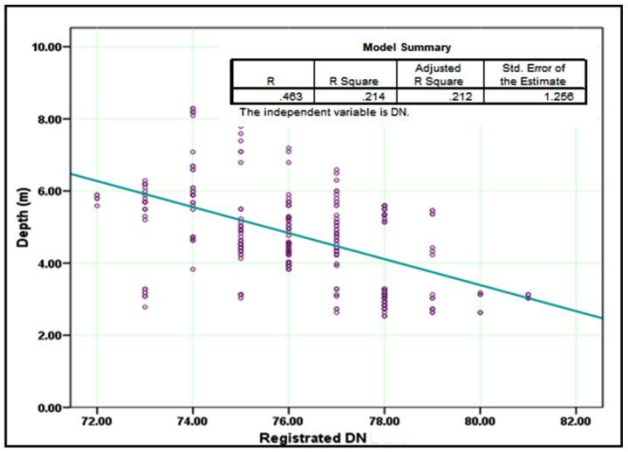

Figure 3. Raw DN of band1 after rectification

4 REGRESSION ANALYSIS

We can achieve all algorithms for retrieval of seawater depth from Remote Sensing Reflectance into the empirical algorithm. It bases the empirical algorithms on the correlation between band reflectance ratios and water depth. This algorithm works well in Case I waters but is not reliable for Case II waters (Hommer and Carter, 2002).

Since the actual depth values collected, a simple linear regression used to compare measured water depths from field to pixel reflectance values in different spectral bands. Note that data were collected from clear water. We can express the simple linear regression model in the following form:

$$D_i = \beta_0 + \beta_1 R_i \qquad (1)$$

where,

D_i is the value of the field measured depth in the i^{th} observation (dependent).

R_i is the reflectance value in the i^{th} observation (independent).

β_0 is the R intercept of the regression line.

β_1 is the slope, and

i=1… n (n represents the number of observations).

Table 3. Different low-pass filters

	Regression values (r^2)								
		3 × 3		5 × 5		7 × 7		9 × 9	
	Raw DN	Low-pass	Reflectance	Low-pass	Reflectance	Low-pass	Reflectance	Low-pass	Reflectance
Band 1	0.632	0.840	0.864	0.876	0.944	0.869	0.894	0.855	0.878
Band 2	0.541	0.669	0.676	0.803	0.862	0.676	0.703	0.640	0.685
Band 3	0.263	0.310	0.360	0.457	0.692	0.391	0.511	0.321	0.450

	Correlations values (r)								
		3 × 3		5 × 5		7 × 7		9 × 9	
	Raw DN	Low-pass	Reflectance	Low-pass	Reflectance	Low-pass	Reflectance	Low-pass	Reflectance
Band 1	0.795	0.916	0.929	0.936	0.971	0.932	0.946	0.925	0.937
Band 2	0.735	0.822	0.822	0.888	0.929	0.822	0.838	0.800	0.828
Band 3	0.513	0.557	0.600	0.676	0.832	0.625	0.715	0.567	0.671

By using SPSS v.15 software, we could derive the estimated model, by estimating the coefficients of model (1) regression coefficients using the data. We plotted scattergrams of reflectance values against depth to select the fitting band for modeling depth (Figures 4, 5 and 6).

We carried the regression analyzes out to test a simple regression relationship between depth and reflectance (bands 1, 2 and 3). We compared the depths derived from a model to the ground truth observations for depths up to 9 m. It was noted, however, that a depth offset of 0.3 m was present between the data sets. The soundings, in the area used, range from less than one meter down to a little over 9 m and are fairly well distributed throughout the range. The total numbers of depth observations taken from this area were 1500 points.

Using the relationship between depth measurements and reflectance for visible bands, we created a model with the slope and intercept of the regression. We found this model that there is a general decrease in bands' reflectance values with an increase in sea depths. We show the results for the regression analysis in table 4 and the resultant model equation created from Band 1 reflectance and actual depth was: $\hat{D} = -633.08 * R + 124.49$, the resultant model created from Band 2 data was: $\hat{D} = -254.81 * R + 48.52$, also for band 3 was $\hat{D} = -480.21 * R + 76.29$. The models were more accurate and fit well with an R^2 of 0.944 for the band 1, an R^2 of 0.863 for the band 2 and an R^2 of 0.692 for the band 3. The coefficients of regression and correlation between the band (one) reflectance and the actual measures represent the highest value. Thus, band 1, offering the highest coefficient of correlation, regression, and it represent the best band used in modeling the water bathymetry. The clear water model for this cause was more accurate with correlation coefficient of 0.971 for depths up to 9 m. We applied results from the regression for band 1 to the Landsat-7 (ETM+) reflectance image, producing an estimated depth image by using ERDAS Spatial Modeler. We present the estimated depths prediction in table 5. The achievement of regression equations is for the structure of condition for the examining area into the configuration of this algorithm. However, some note that there is significant observable relationship between the reflectance (band 1) and field depths data. The correlation has significance at the 0.05 level and the p-value in the analysis of variance shows that the relationship is significant as well. Results from that model showed the potential for this band to be used to extract depth.

5 VALIDITY OF THE MODEL

The regression analyses offered by the model have been verified using data from 1500 new depths locations. Validation results show that a p-value was found significant relationship for the validation test at 95% confidence interval and 0.05, significance level. This validation test model also offered a very good correlation coefficient, 0.9385. As direct scatterplots between actual depths and the independent validation depth by model band 1 are shown in figure 7, give a pure outcome (R^2=0.916). Accordingly, validation model was accepted and ready for used in bathymetry estimation.

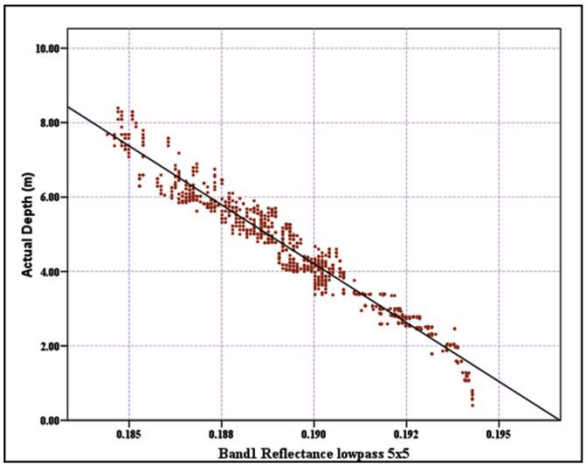

Figure 4. Regression model: Band 1

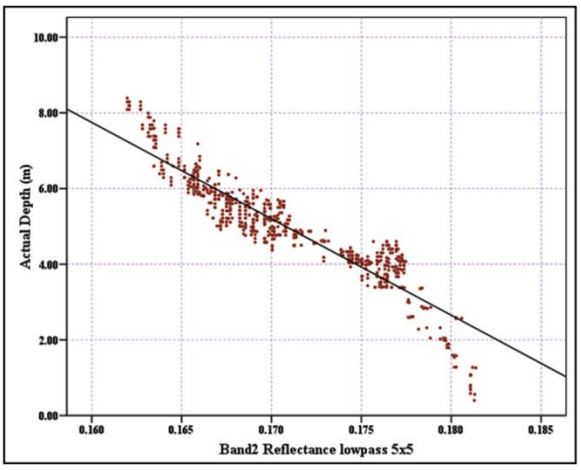

Figure 5. Regression model: Band 2

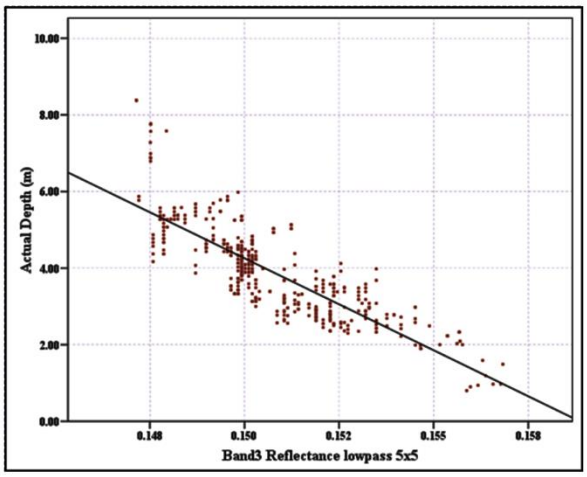

Figure 6. Regression model: Band 3

6 ACCURACY ASSESSMENT

We have calculated the accuracy assessment using the in situ depth data (1500 points) and the estimated depth from the actual depth and pixel reflectance by the regression model algorithm after Louchard *et al.*, (2003):

$$\text{Estimated Error} = \frac{\text{Estimated Depth} - \text{Actual Depth}}{\text{Actual Depth}} \times 100 \quad (2)$$

Both clarity and depth of water affect accuracy. The accuracy of depth values estimated in clear water was 95.92%, while the coefficient of correlation was 0.97 (estimated error = 4.08%). Depth values ranged from less than 1 up to 9 meters. However, when the depth goes over 8 meters, the standard error increases because of the absorption of the electromagnetic wave through the water. Although the models created and the methodologies of field measurements were accurate, still there was minor errors in-depth accuracy as mentioned above (4.08%). These errors need to be overcome since navigation requires high accuracy. To do this a safe factor which should be more than the maximum error recorded must be added or subtracted from depth estimated by the bathymetry models. This will give us a safe range within which the will fall the correct depth.

7 NAVIGATIONAL SAFE FACTOR (PREDICTION INTERVAL)

Since we have the estimated depth based on actual depth and pixel reflectance, then it is essential to extract a new safety depth using safe factor ε. To find the prediction interval, equation (equation 3) has been employed.

$$\hat{D}_{new} \mp t_{\left(\frac{\alpha}{2};n-2\right)} \times S(\hat{D}_{new}) \quad (3)$$

where,

$\hat{D}_{new}$ is the new depth to be predicted.

α is the confidence level.

$S(\hat{D}_{new})$ is the standard deviation of $\hat{D}$ and given by the following formula:

Table 4. Regression analysis

Model summary: Band 1					
	R	R^2	Standard error of estimations		
	0.971	0.944	0.350		
	The independent variable is reflectance.				
	Unstandardized coefficients		Standardized coefficients		
	B	Standard error of estimations	Beta	t	Sig.
Reflectance	-633.078	4.591	-0.971	-137.884	0.000
(constant)	124.492	0.869		143.230	0.000

Model summary: Band 2					
	R	R^2	Standard error of estimations		
	0.929	0.863	0.0484		
	The independent variable is reflectance.				
	Unstandardized coefficients		Standardized coefficients		
	B	Standard error of estimations	Beta	t	Sig.
Reflectance	-254.810	3.225	-0.927	-79.010	0.000
(constant)	48.517	0.551		88.005	0.000

Model summary: Band 3					
	R	R^2	Standard error of estimations		
	0.832	0.692	0.643		
	The independent variable is reflectance.				
	Unstandardized coefficients		Standardized coefficients		
	B	Standard error of estimations	Beta	t	Sig.
Reflectance	-480.207	14.449	-0.832	-33.234	0.000
(constant)	76.286	2.178		35.021	0.000

Table 5. Statistics

No.	Easting	Northing	Reflectance (Band 1)	Field depth	Estimated depths	
					Depth_B1	Difference
1	250342.3301	1740437.6260	0.1847	8.39	8.64	-0.25
2	250386.1760	1740417.4187	0.1848	8.29	8.80	-0.51
3	250392.5692	1740415.3924	0.1848	8.19	8.48	-0.29
4	250406.5601	1740413.6145	0.1848	8.09	8.64	-0.55
5	251944.8562	1742343.7789	0.1846	7.68	7.62	0.06
6	251962.9772	1742322.7864	0.1849	7.38	7.44	-0.06
7	250431.7561	1740390.7900	0.1854	7.09	7.13	-0.04
8	250724.2261	1740381.1096	0.1863	6.69	6.52	0.17
9	251895.7647	1742527.2354	0.1863	6.48	6.52	-0.04
10	251382.5655	1741362.6313	0.1867	6.32	6.27	0.05
11	252126.2749	1742721.5359	0.1875	5.95	5.78	0.17
12	251348.7295	1741213.8861	0.1872	5.82	5.97	-0.15
13	251834.4848	1741588.6504	0.1884	5.26	5.23	0.03
14	252209.3868	1741781.2585	0.1890	5.05	4.86	0.19
15	252393.7784	1741882.3582	0.1892	4.78	4.74	0.04
16	253632.8049	1742058.1626	0.1893	4.43	4.62	-0.19
17	253313.9465	1742370.4044	0.1901	4.20	4.13	0.07
18	253457.1138	1742103.6386	0.1901	4.04	4.13	-0.09
19	253306.9400	1742099.9997	0.1903	3.87	4.01	-0.14
20	253153.0854	1742127.4907	0.1908	3.63	4.12	-0.49
21	251341.6456	1740528.5647	0.1913	3.41	3.37	0.04
22	252049.7234	1742100.5403	0.1922	3.00	2.82	0.18
23	251532.0602	1739640.0763	0.1924	2.79	2.70	0.09
24	251592.6829	1740848.8389	0.1926	2.55	2.57	-0.02
25	251476.2902	1740387.8401	0.1935	1.86	2.00	-0.14
26	253526.4420	1740287.8990	0.1942	1.27	1.55	-0.28
27	252724.8510	1740692.9470	0.1943	0.74	1.50	-0.76
28	253299.9430	1740214.8420	0.1943	0.40	1.49	-1.09

$$S^2(\hat{D}_{new}) = MSE\left[\frac{1}{n} + \frac{(R_d - \bar{R})^2}{\sum_{i=1}^{n}(R_i - \bar{R})^2}\right]$$

MSE is the mean square error, R_d is the desired reflectance point e.g. (R = 102), $\bar{R}$ is the average reflectance which equal (0.183).

Example 1: Consider a navigator has estimated depths for certain area and needs to navigate with more safety and security depth under the ship draft. If they wish to predict the new depth at an estimated depth point of 8 m with 95% as confidence level, then apply equation (3) with *MSE* = 0.350 (See table 4) to get a prediction interval.

$$7.230 \le 8 \le 8.770$$

With a confidence prediction of 0.95, the navigator predicts that the maximum depth would not exceed 8.770 meters and the minimum would not go down 7.230 meters. The safe factor would be $\pm$ 0.77 meters. As a navigator responsible for the safety of the crew and the ship it should take the minimum predicted value into consideration. Another approach if the navigator has a list of estimated depths, such as the depths shown on Figure 8, would be to take the maximum error to apply the safety factor, so if he takes the ED of 9.5 m the interval will be:

$$8.730 \le 9.5 \le 10.270$$

So the safe depth for navigator will be 8.730 meters.

8 CONCLUSION

The results show that data from Landsat-7 (ETM+) with 28.50 m pixel size could employ for bathymetry determination (but model results were not valid for depths greater than 8 meters). The analysis has approved that blue band (band 1: 0.45 - 0.52 µm) is the optimum for bathymetry studies. Regression model has been found to fit and offered 94.40 %. Band 1 reflectance exhibits a very high coefficient of correlation value of 97.10% (as approved by validation test).

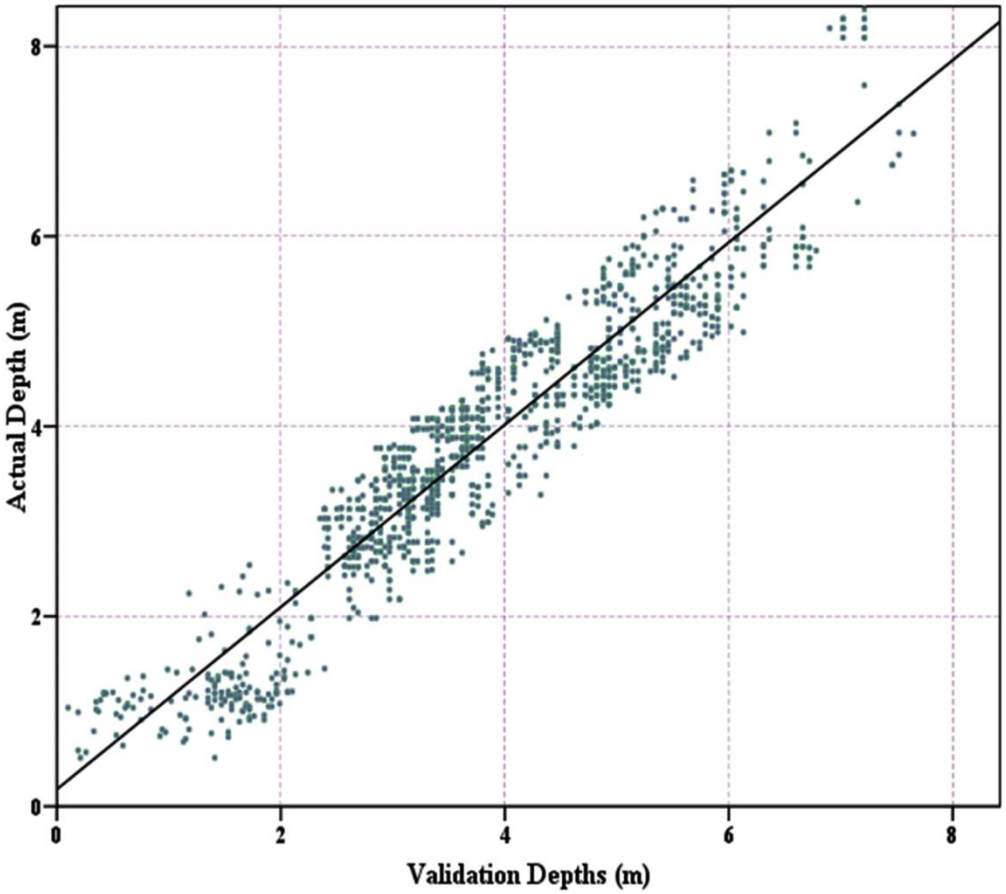

Figure 7. Al-Luhaia regression model for band 1 versus unused actual depth

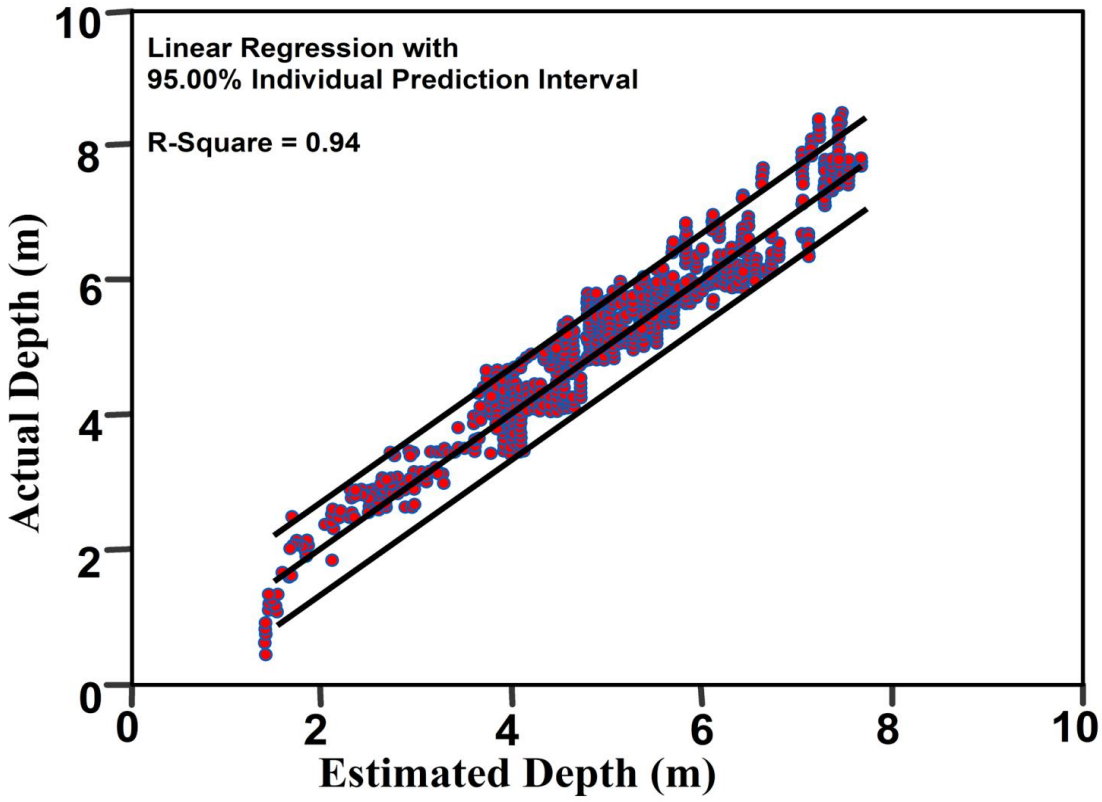

Figure 8**.** Predicted interval of Band 1 for Al-Luhaia area (clear water)

9 DISCUSSION

The mean of bathymetry measures in this work are the usage of low-cost Landsat-7 (ETM+); GPS (locating sampling points); optimum spectral band; accurate least-squares regression link between depth and reflectance value. Blue band (band 1) reflectance was used to feed the regression model. Although Al-Luhaia port was selected as a case study in this paper, some important facts related to band selection, use of GPS and linear regression model approach have emerged, which may apply to many coastal and port areas. Remote sensing has offered very useful bathymetric maps of the Al-Luhaia area and similar maps can be generated for other coastal regions.

The differences in the regression model revealed that the model results were not valid for depths greater than 8 meter for the blue band because of the light diffuse as the depth increase which causes the absorption of light energy which does not encourage result and not support the research aims for updating nautical charts. International Hydrographic Organization (IHO) has set up the accuracy requirements for soundings as 0.3 m for depths up to 30 m, 1 m for depths from thirty to hundred meters, and one percent of the depth, for water depths over 100 m (Baban, 1993). Therefore, this study presented encouraging result which could help in deriving bathymetry maps of shallow coastal areas less than 7.5 m.

ACKNOWLEDGEMENTS

Authors give a great acknowledge to the Egyptian Hydrographic Company (Ehco) and Zone Engineering and Survey who let us join their field trips and donate all marine field survey data for study area. Also, we acknowledge the facilities approved by Port of Al-Hodeida-Yemen, Hydrographic surveying section during this work.

Also, great acknowledge to the Laboratory of Remote Sensing and GIS, Institute of Environmental Studies and Researches, University of Sadat City for providing laboratory facilities and software to accomplish this work.

CONFLICT OF INTEREST

The authors declare no conflict of interest.

ABBREVIATIONS

DGPS: Differential Global Positioning System; **DN**: Digital Number; **ETM**: Enhanced Thematic Mapper; **IHO**: International Hydrographic Organization; **R**: Correlation Value; **USGS**: United States Geological Survey; **WRS**: Worldwide Reference System.

REFERENCES

Abu Daya, M. I., 2004. Coastal water quality monitoring with remote sensing in (East Kalimantan) Makassar Strait, Indonesia, international institute for geo-information science and earth observation Enscheda, the Netherlands, MSc degree.

Andréfouët, S., Muller-Karger, F. E., Hochberg, J. E., Hu, C. and Carder, K. L., 2001. Change detection in shallow coral reef environments using Landsat 7 ETM+ data. *Remote Sensing of Environment*, 78, 150-162. DOI: https://doi.org/10.1016/S0034-4257(01)00256-5

Baban, S. M. J., 1993. The evaluation of different algorithms for bathymetry charting of lakes using Landsat imagery. *International Journal of Remote Sensing*, 14, 2263-2273. DOI: https://doi.org/10.1080/01431169308954035

Benveniste, J., Cazenave, A., Vignudelli, A., Fenoglio-Marc, L., Shah, R., Almar, R., Andersen, O., Birol, F., Bonnefond, P., Bouffard, J., Calafat, F., Cardellach, E., Cipollini, P., Cozannet, G. L., Dufau, c., Fernandes, M. J., Frappart, F., Garrison, J., Gommenginger, C., Han., G., Høyer, J. L.,Kourafalou, V., Leuliette, E., Li, Z., Loisel, H., Madsen, K. S., Marcos, M., Melet, A., Meyssignac, B., Pascua, A., Passaro, M., Ribó, S., Scharroo, R., Song, Y. T., Speich, S., Wilkin, J., Woodworth, P., and Wöppelmann, G., 2019. Requirements for a coastal hazards observing system. *Front. Mar. Sci.* 6, 348. DOI: https://doi.org/10.3389/fmars.2019.00348

Danaher, T. and P. Smith, 1988. Applications of shallow water mapping using passive remote sensing. Proceedings of a Symposium on Remote Sensing of the Coastal Zone, Gold Coast, Queensland, 7 - 9 September 1988, 7.

Diaz, H., Almar, R., Bergsma, E. W. J., Leger, F., 2019. On the use of satellite-based digital elevation models to determine coastal topography. In Proceedings of the IGARSS 2019, IEEE International Geoscience and Remote Sensing Symposium, Yokohama, Japan, 28 July-2 August 2019.

George, D. G., 1997. Cover bathymetric mapping using a compact airborne spectrographic imager (CASI). *International Journal of Remote Sensing*, 18, 2067-2071. DOI: https://doi.org/10.1080/014311697217756

Gordon, H. R. and Brown, O. B., 1974. Influence of bottom depth and albedo on the diffuse reflectance of a flat homogeneous ocean. *Applied Optics*, 13, 2153-2160. DOI: https://doi.org/10.1364/AO.13.002153

Gould Jr. R.W. and Arnone, R. A., 1997. Remote sensing estimates of inherent optical properties in a coastal environment. *Remote Sensing of Environment*, 61 (2), 290-301. DOI: https://doi.org/10.1016/S0034-4257(97)89496-5

Herlevi, A., 2002. A study of scattering, backscattering and a hyperspectral reflectance model for boreal waters. *Geophysica*, 38 (1-2), 113-132.

Hesselmans, G. H, F. M., Wensink, G. J., Van. Koppen, C. G., Vernemmen, C. and Van. Cauwenberghe, C., 2000. Bathymetry assessment demonstration off the Belgian Coast-Babel. *The hydropgraphic Journal*, 96, 3-8.

Hesselmans, G., Calkoen, C. and Wensink, H., 1997. Mapping of seabed topography to and from synthetic aperture radar. In 3rd ERS Symposium on Space at the Service of the Environment (ed. ESA), 1055-1058. Florence, Italie.

Hochberg, E. J., Atkinson, M. J. and Andréfouët, S., 2003. Spectral reflectance of coral reef bottom-types worldwide and implications for coral reef remote sensing. *Remote Sensing of Environment* 85, 159-173. DOI: https://doi.org/10.1016/S0034-4257(02)00201-8

Holden, H. and LeDrew, E., 1998. Spectral discrimination of healthy and non-healthy corals based on cluster analysis, principal components analysis and derivative spectroscopy. *Remote Sensing of Environment*, 65, 217-224. DOI: https://doi.org/10.1016/S0034-4257(98)00029-7

Holden, H. and LeDrew, E., 2002. Measuring and modeling water column effects on hyperspectral reflectance in a coral reef environment. *Remote Sensing of Environment*, 81 (2-3), 300-308. DOI: https://doi.org/10.1016/S0034-4257(02)00007-X

Hommer, D., Carter, C. and Liu, Q., 2002. Ocean color/chlorophyll, visible imager/radiometer suite algorithm theoretical basis document. Version 5, Revision 1. Kendal Carder, Science Team Member, University of South Florida. 56. Accessed on Januray 2003.

Ibrahim, M. and Craclrneil, A. P., 1990. Cover bathymetry using Landsat MSS data of Penang Island in Malaysia. *International Journal of Remote Sensing*, 2, 557-559. DOI: https://doi.org/10.1080/01431169008955040

Ji, C. Y., 2008. Haze reduction from the visible bands of LANDSAT TM and ETM+ images over a shallow water reef environment. *Remote Sensing of Environment*, 112 (4), 1773-1783. DOI: https://doi.org/10.1016/j.rse.2007.09.006

Kumar, V. K., Palit, A., and Bhan, S. K., 1997, Cover bathymetric mapping in Rupnarayan–Hooghly river conuence using IRS data. *International Journal of Remote Sensing*, 18, 2269-2270. DOI: https://doi.org/10.1080/014311697217585

Lafon, V., Castaing, P., Froidefond, J. M. and Lahet, F., 2002. SPOT shallow water bathymetry of a moderately turbid tidal inlet based on field measurements. *Remote Sensing of Environment*, 81(1), 136-148. DOi: https://doi.org/10.1016/S0034-4257(01)00340-6

Li-Guang, L., Heng-Wen, C., 2005. Remotely sensing in detecting the water depths and bed load of shallow waters and their changes. *Ocean Engineering*, 32, 1174-1198. DOI: https://doi.org/10.1016/j.oceaneng.2004.12.005

Louchard, E. M., Reid, R. P., Stephens, F. C., Davis, C. O., Leathers, R. A. and Downes, T. V., 2003. Optical remote sensing of benthic habitats and bathymetry in coastal environments at Lee Stocking Island, Bahamas: A comparative spectral classification approach. *Limnology and Oceanography*, 48(1), 511-521. DOI: https://doi.org/10.4319/lo.2003.48.1_part_2.0511

Lubin, D., Li, W., Dustan, P., Maze, C. H. and Stamnes K., 2001. Spectral signatures of coral reefs: Features from space. *Remote Sensing of Environment*, 75, 127-137. DOI: https://doi.org/10.1016/S0034-4257(00)00161-9

Luczkovich, J. J., Wagner, T. W., Michalek, J. L. and Stoffle, R.W., 1993. Discrimination of coral reefs, seagrass meadows, and sandy bottom types from space: A Dominican Republic case study. *Photogrammetric Engineering and Remote Sensing*, 59(3) 385-389.

Lundahl, A. C., 1948. Underwater depth determination by aerial photography. *Photogrammetric Engineering*, 14(4), 454-462.

Lyzenga, D. R., 1978. Passive remote-sensing techniques for mapping water depth and bottom features. *Applied Optics*, 17(3), 379-383. DOI: https://doi.org/10.1364/AO.17.000379

Mobley, C. D., 1994. *Light and Water; Radiative Transfer in Natural Waters*. Academic Press, Inc., San Diego, CA.

Mumby, P. J., Skirving, W., Strong, E. A., Hardy, J. T., LeDrew, E. F., Hochberg, E. J., Stumpf, R. P., and David, L. T., 2004 . Remote sensing of coral reefs and their physical environment. *Marine Pollution Bulletin*, 48, 219-228. DOI: https://doi.org/10.1016/j.marpolbul.2003.10.031

Pang, L., Zhang M.-B., Zhang J.-X., Zheng Z.-Q., Lin Z.-J., 2004. Shallow seawater depth retrieval based on bottom classification from remote sensing imagery. *Chinese Geographical Science*, 14(3), 258-262. DOI: https://doi.org/10.1007/s11769-003-0056-x

Polcyn, F. C., and Lyzenga, D. R., 1979. Landsat bathymetric mapping by multispectral processing. Proceedings of T hirteenth International Symposium on Remote Sensing of Environment (Ann Arbor, MI: ISPRS), 1269-1276.

Roberts, A. C. B. and Anderson, J. M., 1999. Shallow water bathymetry using integrated airborne multi-spectral remote sensing. *International Journal of Remote Sensing*, 20(3), 497-510. DOI: https://doi.org/10.1080/014311699213299

Sandidge, J. C., Holyer, R. J., 1998. Coastal bathymetry from hyperspectral observation of water radiance. *Remote Sensing of Environment*, 65 (3), 341-352. DOI: https://doi.org/10.1016/S0034-4257(98)00043-1

Smith, R. C. and Baker, K. S., 1981. Optical properties of the clearest natural waters (200-800nm). *Applied Optics*, 20, 177-184. DOI: https://doi.org/10.1364/AO.20.000177

Stove, G. C., 1985. Use of high-resolution satellite imagery in optical and infrared wavebands as an aid to hydrographic and coastal engineering. Proceedings Conference on Electronics in Soil and Gas, London, January *1985* (Twickenham, UK: Cahners Exhibitors), 509-530.

Stumpf, R. P., Holderied, K. and Sinclair, M., 2003. Determination of water depth with high-resolution satellite imagery over variable bottom depths. *Limnology and Oceanography*, 48, 547-556.

Tripathi, N. K., and Rao, A. M., 2002. Bathymetric mapping in Kakinada Bay, India, using IRS-1D LISS-III Data. *Int. J. Remote Sensing*, 23(6), 1013-1025. DOI: https://doi.org/10.1080/01431160110075785

Warne, D. K., 1972. Landsat as an aid in the preparation of hydrographic charts. *Photogrammetric Engineering and Remote Sensing*, 44, 1011-1016.

Woodruff, D. L., Paerl, H. W., Stumpf, R. P. and Scope, J. A., 1999. Remote sensing of water clarity in optically complex estuarine waters. *Remote Sensing of Environment*, 68(1), 41-52. DOI: https://doi.org/10.1016/S0034-4257(98)00108-4

Wu, D., Du, Y., Su, F., Huang, W. and Zhang, L., 2018. An improved DEM construction method for mudflats based on BJ-1 small satellite images: A case study on Bohai Bay. *ISPRS Int. Arch. Photogramm. Remote Sens. Spat. Inf. Sci.*, 1871-1878. DOI: https://doi.org/10.5194/isprs-archives-XLII-3-1871-2018

Yamano, H. and Tamura, M., 2004. Detection limits of coral reef bleaching by satellite remote sensing: Simulation and data analysis. *Remote Sensing of Environment*, 90, 86-103. DOI: https://doi.org/10.1016/j.rse.2003.12.005

Yi, G., and Li, T., 1988. The ocean information contents of remotely sensed image and the acquisition of water depth message. Proceedings of the Ninth Asian Conference on Remote Sensing, Bangkok, Thailand (Asian Association of Remote Sensing, University of Tokyo, Japan), F-3-1-F-3-8.

Zainal, A. J. M., Dalby, D. H. and Robinson, L. S., 1993. Monitoring marine ecological changes on the East Coast of Bahrain with Landsat TM. *Photogrammetric Engineering and Remote Sensing*, 59(3), 415-421.

*****